



Published in final edited form as:

*Med Phys.* 2005 June ; 32(6): 1524–1528.

## Sensitive and fast $T_1$ mapping based on two inversion recovery images and a reference image

Geon-Ho Jahng<sup>a</sup>, Lara Stables, Andreas Ebel, Gerald B. Matson, Dieter J. Meyerhoff, Michael W. Weiner, and Norbert Schuff

University of California-San Francisco, 4150 Clement Street, 114M San Francisco, California 94121

### Abstract

We developed a fast method to obtain  $T_1$  relaxation maps in magnetic resonance imaging (MRI) based on two inversion recovery acquisitions and a reference acquisition, while maintaining high sensitivity by utilizing the full dynamic range of the MRI signal. Optimal inversion times for estimating  $T_1$  in the human brain were predicted using standard error propagation theory. *In vivo* measurements on nine healthy volunteers yielded  $T_1$  values of  $1094 \pm 18$  ms in gray matter and  $746 \pm 40$  ms in white matter, in reasonable agreement with literature values using conventional approaches. The proposed method should be useful for clinical studies because the  $T_1$  maps can be obtained within a few seconds.

### Keywords

MRI; spin lattice relaxation time; inversion recovery; error propagation

## I. INTRODUCTION

Spin-lattice relaxation times ( $T_1$ ) measured with magnetic resonance imaging (MRI) can provide important information about normal and pathological conditions. Furthermore, various MRI applications, such as arterial spin labeling perfusion imaging,<sup>1,2</sup> magnetization transfer imaging,<sup>3</sup> and temperature monitoring<sup>4</sup> require estimates of  $T_1$  for quantification. A large number of different methods have been proposed to measure  $T_1$  relaxation (for an extensive review see Refs. 5 and 6). Conventionally, an inversion recovery (IR) experiment is repeated with multiple inversion times to estimate  $T_1$ .<sup>7</sup> This approach requires relatively long scan times and may compromise accuracy because of involuntary subject motion during data acquisition. In addition, the precise timing of the negative-to-positive zero crossing of the IR signal is usually not easily identified in conventional MRI, because in general only magnitude images are stored. Finally, multi-time point methods are generally very sensitive to image noise, especially at inversion times (TI) where the signal is close to zero ( $TI > T_1 * \ln 2$ ).<sup>8</sup>

To reduce these problems, several two-point methods were introduced to measure  $T_1$  using either a combination of saturation-recovery (SR) and IR spin preparations,<sup>8,9</sup> or two different repetition times, or two different pulse flip angles without SR and IR preparations.<sup>10,11</sup> However, these methods have certain limitations. If a combination of SR and IR spin preparation is used, dynamic range is sacrificed, because SR experiments yield only 50% of the signal range of IR experiments. Moreover, differences in rf power between SR and IR pulses can introduce systematic errors for  $T_1$  measurements. If different repetition times or flip angles are used, dynamic range is also reduced and/or systematic errors in  $T_1$  can be introduced

<sup>a</sup> Electronic mail: ghjahng@itsa.ucsf.edu.

by deviations of actual flip angles from their nominal settings. Dependency on flip angles is also a problem for inversion recovery methods using a Look–Locker acquisition,<sup>12</sup> which furthermore diminishes signal-to-noise ratio because fast repetitions of excitation pulse are employed.

The primary objective of this study was to develop a method for  $T_1$  mapping based on two IR images and a reference image, thus allowing the maximum measurement dynamic range to be used within a very short scan time. Another objective was to eliminate complications with zero crossing of the signal for  $T_1$  measurements. Using single-shot echo planar imaging (EPI) (Ref. 13) to further reduce scan time, multislice  $T_1$  maps of human brain were obtained within a few seconds.

## II. THEORY

The magnetic resonance signal,  $S_e$ , of a single-shot gradient-echo (GE) EPI sequence at echo time TE with repetition time, TR ( $TR \gg T_1$  of brain tissue) can be expressed as  $S_e = S_0 \exp(-TE/T_2^*)$ , where  $S_0$  is the initial equilibrium magnetization and  $T_2^*$  is the transverse relaxation time due to both random magnetic field fluctuations and static magnetic susceptibility. If an inversion pulse is applied prior to the GE-EPI acquisition, the signal is then subject to  $T_1$  relaxation for an inversion time TI, according to

$$S_{IR}(TI) = S_e \left[ 1 - (1 - k) \exp\left(-\frac{TI}{T_1}\right) \right], \tag{1}$$

where  $k = \cos(\alpha_{eff})$  accounts for imperfect inversion by a pulse with effective flip angle  $\alpha_{eff}$ .<sup>6</sup> Note that full relaxation is assumed ( $TR >$  seven times the  $T_1$  of brain tissue). To estimate  $T_1$ , at least two measurements at two different inversion times  $TI_1$  and  $TI_2$  are required. From the two measurements shown in Fig. 1, yielding  $S_{IR1}$  at  $TI_1$  and  $S_{IR2}$  at  $TI_2$ , two difference signals,  $S_e - S_{IR1}$  and  $S_e - S_{IR2}$ , can be obtained. By taking their ratios  $(S_e - S_{IR1}) / (S_e - S_{IR2})$ , and rear-ranging the components,  $T_1$  can then be estimated from the expression

$$T_{1m} = \frac{TI_2 - TI_1}{\ln\left(\frac{S_e - S_{IR1}}{S_e - S_{IR2}}\right)}, \tag{2}$$

with  $T_{1m}$  indicating an estimated value of  $T_1$ . By taking the ratio  $(S_e - S_{IR1}) / (S_e - S_{IR2})$ , the  $(1 - k)$  term disappears, achieving insensitivity to inversion pulse imperfections.<sup>6</sup> Note, standard MR acquisitions produce magnitude images only, but since it is obvious that spins must have a negative magnetization at the shortest  $TI_1$ , the sign of  $S_{IR1}$  can be reversed in Eq. (2) to gain the full range of magnetization, as shown in Fig. 1.

To minimize the error in computing  $T_{1m}$  of gray and white matter in the human brain, first-order error propagation theory was applied to determine an optimum combination of  $TI_1$  and  $TI_2$  values, assuming a perfect inversion rf pulse. With the assumption that the measurement errors of  $S_{IR1}$ ,  $S_{IR2}$ , and  $S_e$  are uncorrelated and that each has the same standard of deviation ( $\sigma_S$ , the standard of deviation of the error in the  $T_{1m}$  measurement,  $\sigma_{T_{1m}}$ , is

$$\frac{\sigma_{T_{1m}}}{T_1} \left( \frac{1}{2} \right) \left( \frac{\sigma_S}{S_e} \right) \left( \frac{T_1}{TI_2 - TI_1} \right) \times \left\{ \frac{\sqrt{\exp(-2 \cdot TI_2/T_1) + \exp(-2 \cdot TI_1/T_1)}}{\exp[-(TI_1 + TI_2)/T_1]} \right\}. \tag{3}$$

The derivation of first-order error propagation for Eq. (3) can be found in references by Kurland<sup>8</sup> and Imran *et al.*<sup>10</sup> Obviously,  $TI_2$  must be different from  $TI_1$  to avoid a singularity

from the  $1/(TI_2 - TI_1)$  term in Eq. (3). On the other hand, their difference should not be too large, because  $1/(TI_2 - TI_1)$  is counterbalanced by  $1/\exp(-(TI_1 + TI_2)/T_1)$ , indicating that the error increases if the signal-to-noise ratio (SNR) of the second IR measurement becomes too small as  $TI_2$  increases. From Eq. (3), the SNRs of  $T_{1m}$  and  $S_e$  are defined as  $SNR_{T_1} = T_1/(\sigma_{T_{1m}})$  and  $SNR_{S_e} = S_e/(\sigma_S)$ , respectively.<sup>14</sup> Equation (3) also implies that if  $T_1$  of gray matter and white matter are roughly known *a priori*,  $TI_1$  and  $TI_2$  values can be carefully optimized to maximize  $SNR_{T_1}$  in human brain.

### III. METHODS

#### A. Simulations

From Eq. (3) it is obvious that  $TI_1$  should be as short as possible. To determine the optimal inversion time of  $TI_2$  for human brain  $T_1$  measurements, computer simulations were performed to evaluate Eq. (3) with the following parameters:  $SNR_{S_e} = 50$  and  $T_1 = 980$  ms (Ref. 7) for gray matter and  $SNR_{S_e} = 30$  and  $T_1 = 640$  ms (Ref. 7) for white matter in human brain at 1.5 T. The  $SNR_{S_e}$  values are typical for the single-shot GE-EPI acquisitions described below. Optimized values found for  $TI_1$  and  $TI_2$  were then used in studies with normal volunteers to measure the pixel-wise  $T_{1m}$  of brain tissue. The simulations were performed using MATHEMATICA software (Wolfram Research, Champaign, IL).

#### B. Experiments in human brain

In order to minimize motion artifacts and noise differences between measurements, a sequence was developed to obtain three sets of images in a single scan using a series of 2D multislice EPI data acquisitions, as shown in Fig. 2. Here,  $180^\circ$  indicates a nonselective inversion pulse;  $90^\circ$  indicates a slice-selective  $90^\circ$  sinc-shaped pulse with duration of 2.56 ms. TE is the echo time between the  $90^\circ$  pulse and the center of EPI  $k$  space. Each slice is acquired with a 52 ms single-shot GE-EPI readout. TD is a variable delay time to maintain a constant TR for all three acquisitions [ $TR = \text{slices} * (TE + EPI/2) + TD_0 = TI_{1 \text{ or } 2} + \text{slices} * (TE + EPI/2) + TD_{1 \text{ or } 2}$ ]. The first image acquisition, which provides the reference image used to calculate  $S_e$ , does not involve an IR-preparation rf pulse. The second and third acquisitions are identical to the first except that a non-selective hyperbolic secant inversion pulse (12.8 ms duration,  $50 \mu T$  of  $B_1$  field strength) was applied to invert spins on the whole volume of interest, followed by multislice acquisitions with two different inversion times,  $TI_1$  and  $TI_2$ . In all three acquisitions,  $TR = 7000$  ms (about seven times  $T_1$  in gray matter) and  $TE = 15$  ms.

To demonstrate the utility of this approach for the *in vivo*  $T_{1m}$  measurement, nine normal volunteers (mean age and standard deviation =  $61 \pm 15$  years and age range = 37–80 years) were studied using a 1.5 T MR system (Vision, Siemens, Germany). A circularly polarized head coil was used for radio frequency transmission and reception. Seven  $8 \text{ mm}$  thick slices with a  $3.4 \times 3.4 \text{ mm}^2$  in-plane resolution and a  $2 \text{ mm}$  gap were acquired in an interleaved fashion to minimize cross-talk effects between slices. The bottom slice was located 1 cm above the Circle of Willis for all subjects. Inversion times of  $TI_1 = 40$  ms and  $TI_2 = 900$  ms were chosen based on simulation results. The total acquisition time for seven slices was 21 s. The  $T_{1m}$  value for each pixel was calculated using Eq. (2).

Regions of interest (ROIs) of gray matter and deep white matter in each subject were selected in the four slices (3 to 6) of the  $S_e$  (reference) images using the OSIRIS software package (Geneva University Hospital, Geneva, Switzerland; <http://www.sim.hcuge.ch>). The gray and white matter  $T_1$  values for each subject were obtained by averaging over these ROIs. Note that images from the subjects were not normalized into a standard space; therefore, the size and anatomical locations of the ROIs used to obtain  $T_1$  values were different for each subject. Representative ROIs are shown in Fig. 4.

## IV. RESULTS

### A. Simulations

$\text{SNR}_{T_1}$ , calculated according to Eq. (3), is plotted in Fig. 3 as a function of  $\text{TI}_1$  and  $\text{TI}_2$  for gray matter (A) and white matter (B). With longer  $\text{TI}_1$ , the  $\text{SNR}_{T_1}$  for gray matter and white matter decreased, indicating that the shortest possible  $\text{TI}_1$  (in this case, 40 ms) should be used. With  $\text{TI}_1 = 40$  ms, the maximum  $\text{SNR}_{T_1}$  was achieved,  $\text{TI}_2 = 1100$  ms for gray matter and  $\text{TI}_2 = 700$  ms for white matter. For the *in vivo* studies, it was decided to use the average of the optimal  $\text{TI}_2$  inversion times for gray and white matter, which was 900 ms.

### B. Studies on human brain

Figure 4 shows single shot GE-EPI ( $S_e$ ) images and corresponding  $T_{1m}$  maps from seven axial sections through the brain of a volunteer. Overall, the  $T_{1m}$  maps show reasonable contrast between gray and white matter. Results of  $T_{1m}$  estimates averaged over gray matter and white matter, respectively, from nine volunteer studies are listed in Table I. Averaged over all subjects, the proposed method yielded  $T_{1m}$  values of  $1094 \pm 18$  ms for gray matter and  $746 \pm 40$  ms for white matter.

## V. DISCUSSION

We have demonstrated that a new acquisition method with carefully selected values of two inversion times provides maps of  $T_1$  estimates of gray matter and white matter that are comparable to those obtained from a phase-sensitive multi-point inversion recovery technique.<sup>7</sup> Compared to published two-point methods for  $T_1$  measurements,<sup>8–11</sup> the proposed method has several advantages: (1) The method makes use of the full dynamic range of both  $S_{IR1}$  and  $S_{IR2}$ , which should improve the SNR (Ref. 15) and therefore improve accuracy for  $T_1$  measurements. (2) By choosing  $\text{TI}_1$  and  $\text{TI}_2$  so that reasonable assumptions can be made about the signs of  $S_{IR1}$  and  $S_{IR2}$ , the problem of identifying the negative-to-positive zero crossing of the IR signal is avoided, because both  $(S_e - S_{IR1})$  and  $(S_e - S_{IR2})$  always yield positive values.<sup>16</sup> However, the proposed method has several limitations: Because nonselective inversion pulses are used, successive slices have different  $\text{TI}_1$ 's and  $\text{TI}_2$ 's. Therefore, although  $\text{TI}_2 - \text{TI}_1$  remains the same for all slices, not all slices will have the optimal inversion time for the highest  $\text{SNR}_{T_1}$  and the dynamic range will decrease for successive slices. In addition, different slices will sample a different part of the relaxation curve, allowing accurate estimation of only monoexponential relaxation. To the extent that longitudinal relaxation in the human brain tissue is multiexponential, including effects due to partial volumes of gray matter, white matter, and CSF, slice-dependent errors in estimating  $T_1$  are introduced. Especially, when data acquisition occurs on a later part of a multiexponential curve,  $T_1$  will appear prolonged. The presence of partial volumes of brain tissue with CSF may have contributed to slightly higher  $T_1$  values in gray and white matter in this study than previously reported. Partial volume effects can be reduced with the acquisition of a higher resolution multishot EPI sequence.

Finally, one should note that the optimized parameters for measuring  $T_1$  of brain tissue result in an underestimation of the  $T_1$  of CSF by about a factor of 4 compared to a value of 4500 ms obtained with a multipoint inversion recovery technique.<sup>14</sup>  $T_1$  of CSF in this study was  $1020 \pm 65$  ms. The proposed technique, therefore, cannot accurately measure  $T_1$  values for brain tissues and CSF with a single set of inversion times  $\text{TI}_1$  and  $\text{TI}_2$  because we do not obtain phase information of inverted spins. Therefore, to accurately measure  $T_1$  of CSF with this approach, the second inversion time of the sequence needs to be adjusted for CSF and a separate dataset acquired. In contrast to brain tissue,  $T_1$  measurements of CSF are accurate for  $\text{TI}_2$  values of about 5 s. However, a  $\text{TI}_2$  of 5 s is no longer optimal for gray, white, and most other brain tissue.

Because the proposed technique requires only two TI points with a reference EPI scan and no more than a few seconds to map  $T_1$ , this technique should be useful for any clinical study that requires an estimate of the  $T_1$  of brain tissue. In addition, the proposed method is ideally suited for use in combination with EPI-based arterial spin labeling perfusion studies to quantitatively measure cerebral blood flow in brain. The arterial spin labeling perfusion images and a  $T_1$  map can be obtained with the same spatial resolution and similar EPI-related image distortions. Another possibility to derive  $T_{1m}$  from  $S_e$  and  $S_{IR2}$  datasets is to calculate the log transform of the images and compute  $T_{1m}$  according to  $T_{1m} = TI_2 / \ln[(1-k)S_e / (S_e - S_{IR2})]$ . However, this method is very sensitive to the selection of the inversion time.

In conclusion, the proposed  $T_1$  measurement based on two IR images utilizes the full dynamic signal range and requires only a few seconds for acquisition, yet yields results similar to those of a conventional method. Therefore, this new method may be useful for obtaining  $T_1$  values of brain tissue in clinical studies, where short scan times and simplicity of data processing are imperative.

#### Acknowledgements

We thank Dr. Peter B. Kingsley for valuable comments. This work was supported by NIH/NIAAA Grant Numbers PO1 AA11493 and RO1 AA10788.

#### References

1. Kwong KK, Chesler DA, Weisskoff RM, Donahue KM, Davis TL, Ostergaard L, Campbell TA, Rosen BR. MR perfusion studies with  $T_1$ -weighted echo planar imaging. *Magn Reson Med* 1995;34:878–887. [PubMed: 8598815]
2. Jahng GH, Zhu XP, Matson GB, Weiner MW, Schuff N. Improved perfusion-weighted MRI by a novel double inversion with proximal labeling of both tagged and control acquisitions. *Magn Reson Med* 2003;49:307–314. [PubMed: 12541251]
3. Wolff SD, Balaban RS. Magnetization transfer contrast (MTC) and tissue water proton relaxation *in vivo*. *Magn Reson Med* 1989;10:135–144. [PubMed: 2547135]
4. Dickinson RJ, Hall AS, Hind AJ, Young IR. Measurement of changes in tissue temperature using MR imaging. *J Comput Assist Tomogr* 1986;10:468–472. [PubMed: 3700752]
5. Kingsley PB. Signal intensities and  $T_1$  calculations in multiple-echo sequences with imperfect pulses. *Concepts Magn Reson* 1999;11:29–49.
6. Kingsley PB. Methods of measuring spin-lattice ( $T_1$ ) relaxation times: An annotated bibliography. *Concepts Magn Reson* 1999;11:243–276.
7. Cho S, Jones D, Reddick WE, Ogg RJ, Steen RG. Establishing norms for age-related changes in proton  $T_1$  of human brain tissue *in vivo*. *Magn Reson Imaging* 1997;15:1133–1143. [PubMed: 9408134]
8. Kurland RJ. Strategies and tactics in NMR imaging relaxation time measurements. I. Minimizing relaxation time errors due to image noise—the ideal case. *Magn Reson Med* 1985;2:136–158. [PubMed: 3831683]
9. Lai S, Wang J, Jahng GH. FAIR exempting separate  $T_1$  measurement (FAIREST): A novel technique for online quantitative perfusion imaging and multi-contrast fMRI. *NMR Biomed* 2001;14:507–516. [PubMed: 11746944]
10. Imran J, Langevin F, Saint-Jalmes H. Two-point method for  $T_1$  estimation with optimized gradient-echo sequence. *Magn Reson Imaging* 1999;17:1347–1356. [PubMed: 10576720]
11. Parker GJ, Barker GJ, Tofts PS. Accurate multislice gradient echo  $T(1)$  measurement in the presence of nonideal rf pulse shape and rf field nonuniformity. *Magn Reson Med* 2001;45:838–845. [PubMed: 11323810]
12. Mason GF, Chu WJ, Hetherington HP. A general approach to error estimation and optimized experiment design, applied to multislice imaging of  $T_1$  in human brain at 4.1 T. *J Magn Reson* 1997;126:18–29. [PubMed: 9177795]

13. Ordidge RJ, Gibbs P, Chapman B, Stehling MK, Mansfield P. High-speed multislice  $T_1$  mapping using inversion-recovery echo-planar imaging. *Magn Reson Med* 1990;16:238–245. [PubMed: 2266843]
14. Haacke, EM.; Brown, RW.; Thompson, MR.; Venkatesan, R. *Magnetic Resonance Imaging: Physical Principles and Sequence Design*. Chap 4. Wiley; New York: 1999. p. 51-64.
15. Crawley AP, Henkelman RM. A comparison of one-shot and recovery methods in  $T_1$  imaging. *Magn Reson Med* 1988;7:23–34. [PubMed: 3386519]
16. Kim SG, Hu X, Ugurbil K. Accurate  $T_1$  determination from inversion recovery images: Application to human brain at 4 Tesla. *Magn Reson Med* 1994;31:445–449. [PubMed: 8208121]

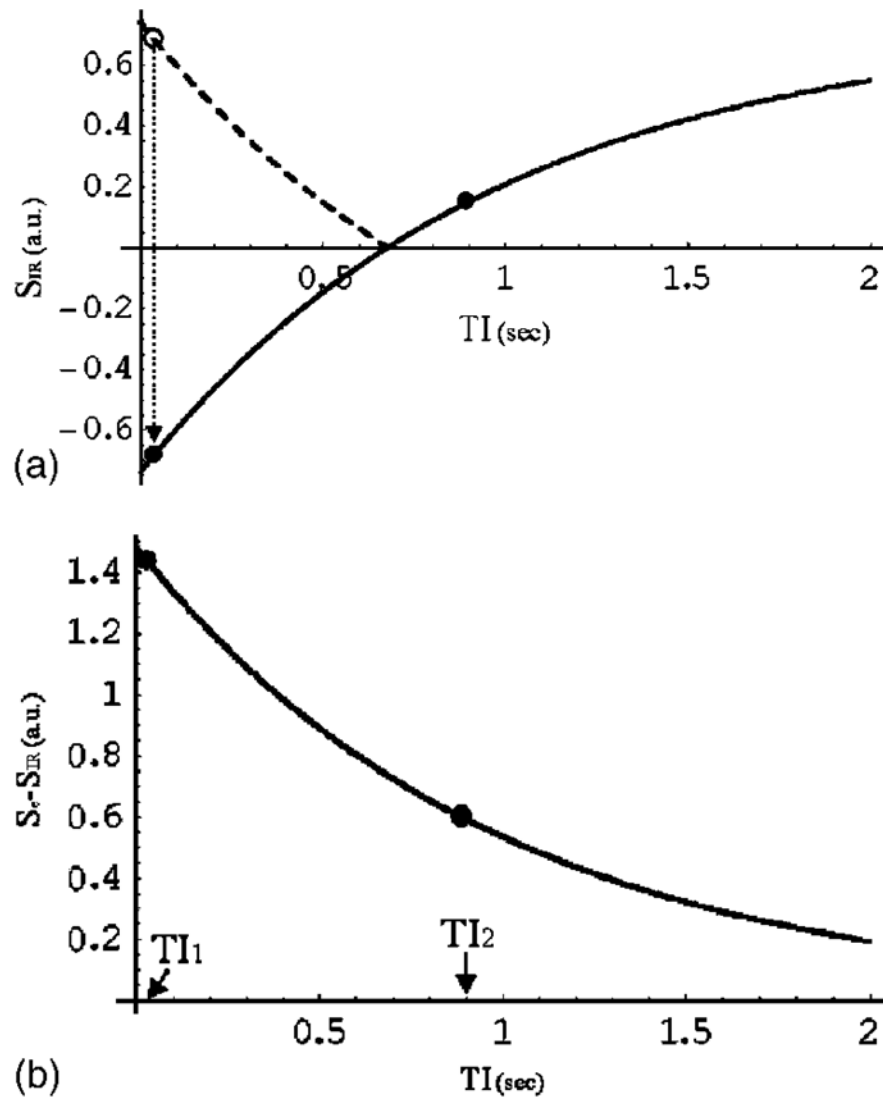


**Fig. 1.** Simulation of the signal intensity of the inversion recovery sequence as a function of inversion time ( $TI$ ) (A) and the difference signal intensity of  $S_e - S_{IR}$  (B). The parameters used were  $TE=15$  ms,  $S_0=1.0$ ,  $T_2^* =50$  ms, and  $T_1 =980$  ms for human gray matter at 1.5 T. In (A), the heavy dashed line before the zero crossing represents the absolute value of  $S_{IR}$ . The two dots represent the inversion times,  $TI_1$  and  $TI_2$ , used to calculate  $T_{1m}$  from the difference signal.

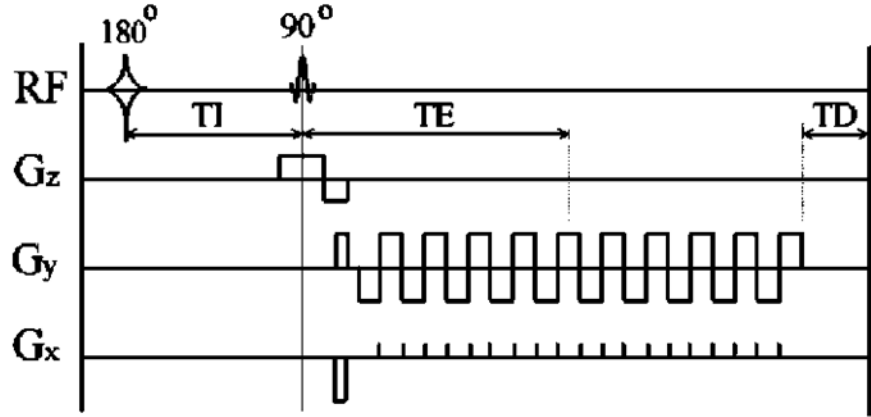


**Fig. 2.** Pulse sequence timing diagram showing radio frequency (rf) pulses and gradients ( $G_r$ ) along each spatial direction  $r=x, y, z$ . A nonselective hyperbolic inversion ( $180^\circ$ ) rf pulse is followed after the inversion time  $TI$  by a slice-selective sinc-shaped excitation ( $90^\circ$ ) pulse.  $G_z$  is the slice selective gradient. An echoplanar image (EPI) is generated by gradients  $G_y$  and  $G_x$ .  $TE$  is the echo time, and  $TD$  is a variable delay time and was adjusted to yield the same repetition time ( $TR=7000$  ms) for all three images. The first image  $S_e$  according to Eq. (2) is obtained without applying a  $180^\circ$  pulse, while the second  $S_{IR1}$  and third  $S_{IR2}$  images are acquired each with a  $180^\circ$  pulse at delays  $TI_1 = 40$  ms and  $TI_2 = 900$  ms, respectively.



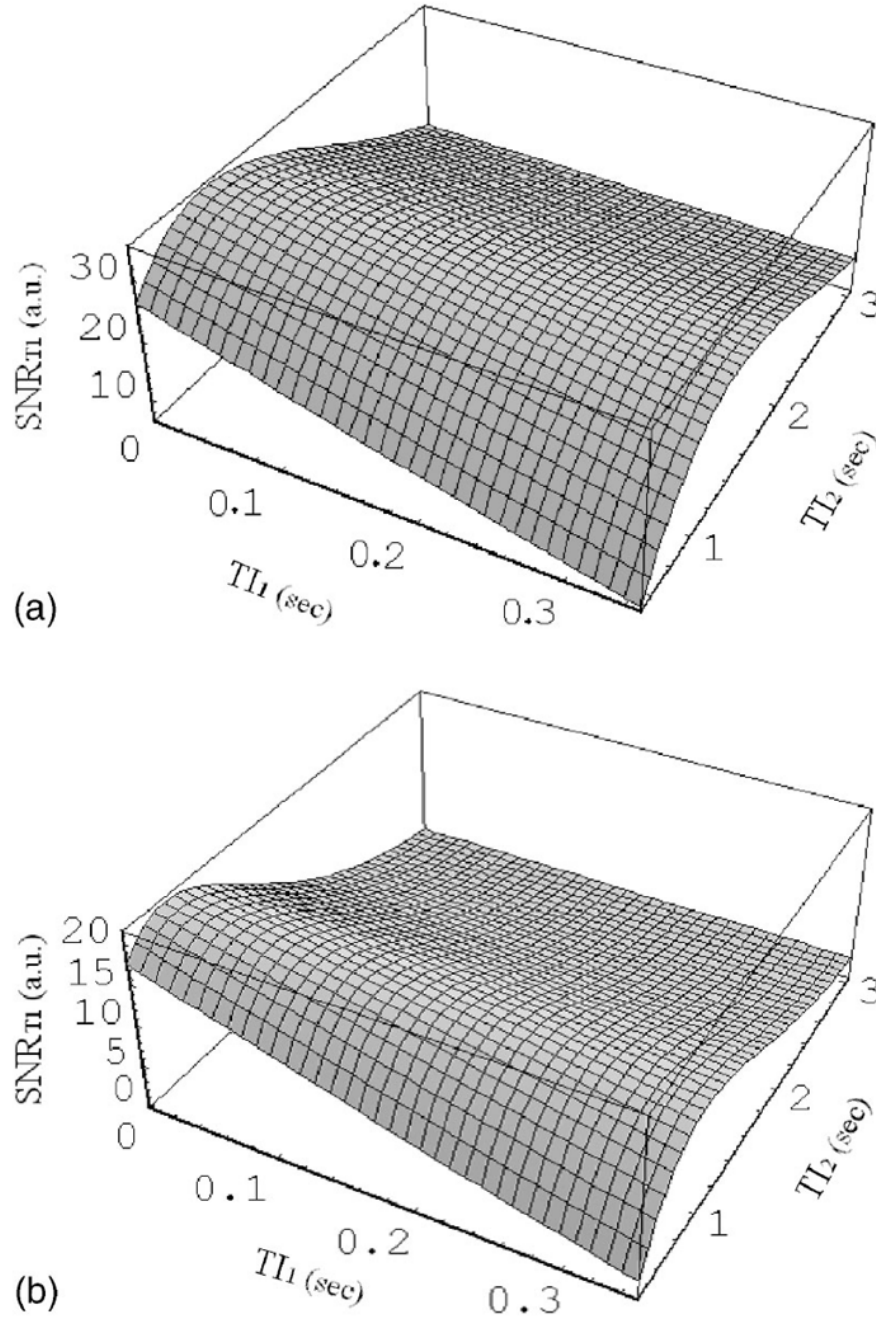


**Fig. 3.** Simulation of  $SNR_{T1}$ , calculated according to Eq. (3), as a function of inversion times  $TI_1$  and  $TI_2$ , assuming a perfect inversion pulse. The simulation parameters used were  $SNR_{Se} = 50$  and  $T_1 = 980$  ms for human gray matter (A) and  $SNR_{Se} = 30$  and  $T_1 = 640$  ms for human white matter (B) at 1.5 T.  $SNR_{T1}$  reached a maximum at  $TI_2 = 1100$  ms for gray matter and at  $TI_2 = 700$  ms for white matter with  $TI_1 = 40$  ms.

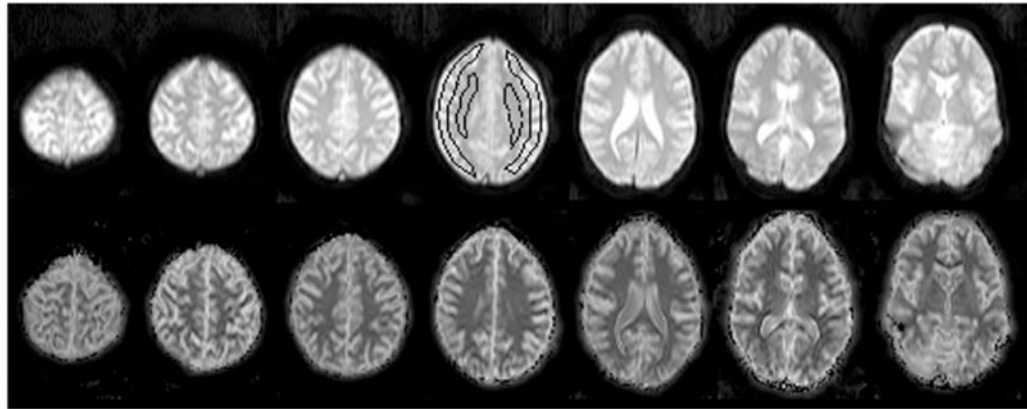


**Fig. 4.** Images from one normal volunteer without inversion preparation (reference  $S_e$  images, top row) and corresponding  $T_{1m}$  maps (bottom row) for seven slices. Representative ROIs of gray matter and white matter were drawn on the middle slice out of seven slices as indicated in the figure. Slices 3 to 6 were used to measure average  $T_1$  values in each subject.

**Table I**

$T_{1m}$  estimates for gray and white matter from nine volunteers.

Subject	Graymatter $T_{1m}$ (ms)	Whitematter $T_{1m}$ (ms)
1	1080±26	720±16
2	1075±55	750±9
3	1100±71	770±8
4	1110±57	703±12
5	1101±68	772±25
6	1090±63	682±33
7	1073±56	730±18
8	1130±82	810±25
9	1090±61	780±23
Mean±STD	1094±18	746±40
Reference <sup>a</sup>	980±63	640±30

<sup>a</sup>Reference from phase-sensitive multipoint inversion recovery sequence published by Cho *et al.* (Ref. 7).